© SEP 2026 | IRE Journals | Volume 10 Issue 3 | ISSN: 2456-8880
DOI: https://doi.org/10.64388/IREV10I3-1723169

Transient Stability Enhancement of the Nigerian 330 kV Interconnected Power Network Using High-Voltage Direct Current (HVDC) Transmission: A Modal Analysis and Time-Domain Simulation Study

VICTOR CHRISTOPHER[1], ISAAC. I. ALABI[2], BEGE HARUNA[3]
[1,2]*Department of Electrical/Electronic Engineering, Nigerian Defence Academy, Kaduna, Nigeria.*
[3]*Department of Computer Engineering Technology, Nuhu Bamalli Polytechnic, Zaria, Kaduna State, Nigeria.*

Abstract- ***The Nigerian 330 kV interconnected transmission network has continued to experience recurrent voltage collapse and system-wide blackouts, a large proportion of which are traceable to poorly damped electromechanical oscillations following large disturbances. This paper presents a systematic modal-analysis-guided approach to transient stability enhancement of the network using a voltage-source-converter-based high-voltage direct current (HVDC) link. A 56-bus representation of the Nigerian 330 kV grid, comprising 15 generator (PV) buses and interconnected by 53 transmission lines, was modelled in a MATLAB/Simulink environment embedded with the Power System Analysis Toolbox (PSAT). The Newton–Raphson power-flow method was used to determine the pre-disturbance operating point of the network, while small-signal (modal) analysis, supported by participation-factor computation, was used to identify the critical inter-area oscillatory mode and the transmission corridor along which it propagates – found to be the Ikeja-West–Benin corridor. An HVDC link was embedded at the identified location and its damping contribution was evaluated through time-domain simulation of a three-phase fault, using the modified Euler (predictor–corrector) method to solve the machine swing equations. Four network parameters – generator rotor speed, bus voltage, and active and reactive line power flows – were monitored with and without the HVDC link. The results show consistent improvement in all four parameters: rotor-speed overshoot reduced by up to 44.4% and settling time by up to 52%; active- and reactive-power oscillation overshoot reduced by up to 100% with settling-time improvement of up to 83.3%; and bus-voltage oscillations were almost completely suppressed, with overshoot reductions of up to 98% and settling-time improvements of up to 95%. The findings confirm that strategically located HVDC, sited using eigenvalue/participation-factor screening rather than heuristic placement, offers a technically robust and readily deployable option for damping inter-area oscillations on the Nigerian grid.***

Keywords: transient stability; HVDC; modal analysis; eigenvalue analysis; participation factor; Newton–Raphson power flow; Nigerian 330 kV grid; inter-area oscillation; time-domain simulation.

I. INTRODUCTION

Modern power systems can be viewed as interconnections of geographically dispersed generators, transformers, transmission lines, substations and loads. As these networks grow in size and are pushed to operate closer to their stability limits – driven by higher loading, wider variety of operating points, and bulk power transfer over long distances – the problems associated with small-signal (oscillatory) stability become increasingly critical for system operators [1], [6]. Transient stability, defined as the ability of a power system to remain in, or return to, an acceptable state of equilibrium following a large disturbance, is one of the principal indices used to assess the security of a network [4].

The Nigerian national grid has, for an extended period, been characterised by recurrent voltage collapse and nationwide blackouts. These events are frequently a secondary consequence of the tripping of synchronous generators occasioned by transient swings that are not adequately damped. It is therefore necessary to provide (i) timely synchronising torque to arrest critical first-swing excursions, and (ii) sufficient power-oscillation damping torque to suppress sustained low-frequency inter-area oscillations before they degrade into instability.

High-voltage direct current (HVDC) transmission, and in particular voltage-source-converter (VSC) based HVDC, is well suited to this dual requirement. Unlike conventional HVAC reinforcement, HVDC allows fast, independent control of active and reactive power, does not increase the prospective short-circuit level of the AC network into which it is embedded, and can rapidly modulate power flow to counteract oscillatory swings [11], [16], [17]. These properties make HVDC an attractive retrofit option for a grid such as Nigeria's 330 kV network, where the corridors most exposed to inter-area oscillation are already identified and where reinforcement by additional AC circuits is often constrained by right-of-way and cost.

A number of prior studies have investigated HVDC-based transient-stability enhancement of the Nigerian grid and similar interconnected systems (Table 1). While these studies establish the general feasibility of HVDC damping control, most of them do not characterise the frequency content of the oscillatory modes being damped, nor do they report how long the oscillations persist before and after compensation – information that is necessary to judge whether a proposed HVDC siting is actually addressing the dominant inter-area mode, or only a secondary, well-damped local mode. This is the gap addressed in this paper.

Accordingly, the aim of this study is the transient-stability enhancement of the Nigerian 330 kV grid using HVDC, with the following objectives: (i) determine the pre-disturbance operating point of the test network; (ii) identify, through modal (eigenvalue) analysis, the critical low-frequency inter-area mode and the transmission corridor that conveys it; (iii) determine the most effective location for an HVDC link using the results of the modal analysis; and (iv) quantify the effectiveness of the HVDC link in enhancing transient stability using time-domain simulation. The remainder of the paper is organised as follows: Section 2 reviews related work; Section 3 presents the test system, the Newton–Raphson power-flow formulation, the modal-analysis and participation-factor formulation, the HVDC dynamic model, and the time-domain (modified Euler) solution method; Section 4 presents and discusses the simulation results; and Section 5 concludes the paper.

II. LITERATURE REVIEW

Eigenvalue-based siting of stability-enhancing devices on the Nigerian 330 kV grid has been explored by several authors. Okolo et al. [25] used eigenvalue analysis to identify unstable buses on the Ajaokuta–Benin corridor and applied an artificial-neural-network (ANN)-tuned VSC-HVDC controller; the method proved feasible, obtaining a stable response, but the resulting damping improvement was modest and the frequency content of the oscillation modes damped was not characterised. Lakshmi and Yuan [31] used an HVDC emergency control circuit that injects a signal 180° out of phase with the oscillation, achieving adequate damping, although the response of the emergency control circuit introduced a noticeable delay. Emmanuel and Ifeanyi [24] applied a similar ANN-tuned HVDC scheme on the considerably shorter Jos–Makurdi line; some improvement in damping was observed, but the short line length limited the extent to which it could meaningfully influence the inter-area oscillation. Sundaresh et al. [20], working on the IEEE 24-bus reliability test system, used HVDC control – modulated by rotor speed, voltage phasor and tie-line power-flow signals through a conventional PI controller – to reduce oscillation magnitude, but achieved only a modest reduction because no optimisation tool was used to reach the maximum achievable damping. Ali et al. [23] carried out a comparative study of HVDC versus HVAC transmission under fault conditions and confirmed that HVDC gives better fault performance than HVAC, but the study was comparative only and did not attempt to maximise the transient-stability improvement obtainable. Relative to these studies, the present work uses Newton–Raphson power flow combined with modal and participation-factor screening to site the HVDC link, followed by time-domain validation, and – unlike the works reviewed above – explicitly identifies the frequency and duration of the oscillatory modes being damped, achieving up to 98% suppression of bus-voltage oscillation and up to 100% overshoot reduction on lightly loaded reactive-power corridors.

© SEP 2026 | IRE Journals | Volume 10 Issue 3 | ISSN: 2456-8880
DOI: https://doi.org/10.64388/IREV10I3-1723169

The studies reviewed above establish that HVDC can contribute to transient-stability enhancement, but none of them explicitly identify the frequency components contained in the oscillation being damped, nor the duration for which the oscillation persists pre- and post-compensation. This paper addresses that gap by combining eigenvalue/participation-factor screening (which yields the modal frequency and damping ratio directly) with time-domain validation (which yields the settling time directly), on the full 56-bus representation of the Nigerian 330 kV grid.

III. MATERIALS AND METHODS

3.1 Test System

The test network is a 56-bus representation of the Nigerian 330 kV interconnected grid, comprising 15 generator (PV) buses and 53 interconnected transmission lines, with one bus designated as the slack bus. The single-line diagram of the network is shown in Figure 1. Bus and line data (voltage magnitude, generation and load schedule, and per-unit line impedance/susceptance) were obtained from PHCN/Energo grid records [3], [34] and are summarised in the appendix of the underlying dissertation on which this paper is based.

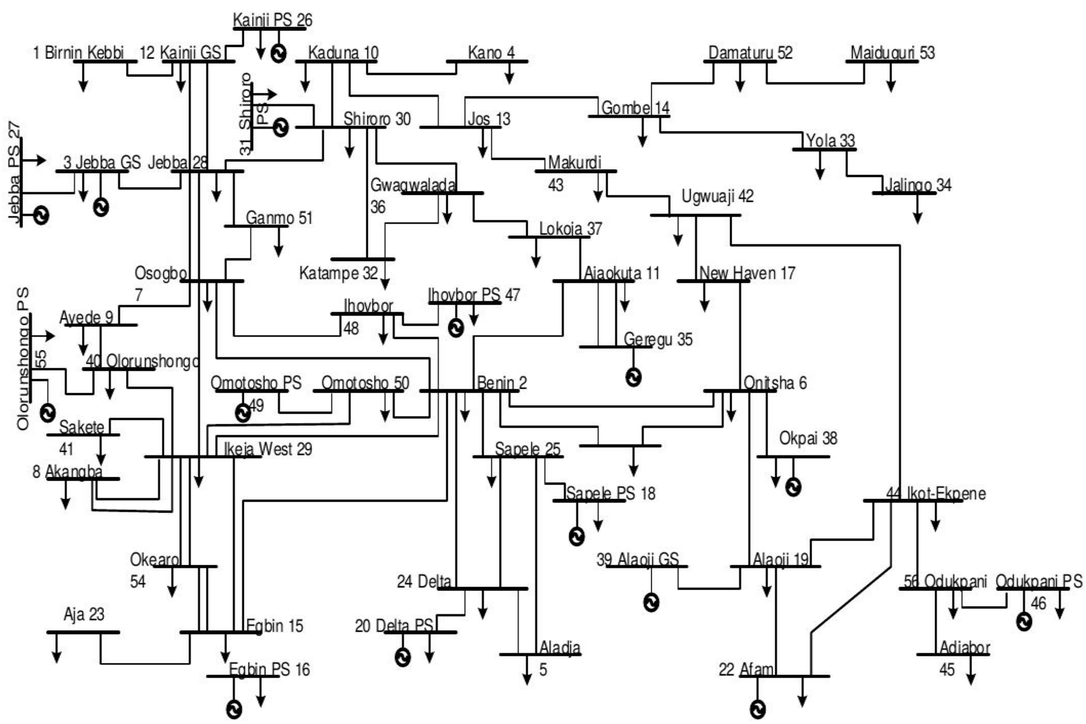

Figure 1: Single-line diagram of the 56-bus Nigerian 330 kV national grid [34].

3.2 Overall Research Methodology

The overall methodology proceeds in the following sequence: (i) the pre-disturbance operating point of the network is obtained by Newton–Raphson power flow; (ii) the network is linearised about this operating point and its eigenvalues, oscillation frequencies and participation factors are computed to identify the critical inter-area mode and the line most strongly associated with it; (iii) the transient response of the un-compensated network to a three-phase fault is obtained by time-domain simulation; (iv) an HVDC link is inserted at the identified line, and steps (ii) and (iii) are repeated; and (v) the damping performance with and without HVDC is compared. This sequence is repeated, varying the candidate line, until the maximum achievable damping improvement is confirmed at the identified critical corridor.

3.3 Newton–Raphson (NR) Power-Flow Formulation

The Newton–Raphson method was adopted for the power-flow solution because of its quadratic convergence and its favourable scaling of memory requirement with network size [10]. At bus i, the injected active and reactive power are

$$P_i = \sum_{\substack{j=1 \\ j\neq i}}^{n} |Y_{ij}||V_i||V_j| \cos(\theta_{ij} + \delta_j - \delta_i) \quad (1)$$

$$Q_i = -\sum_{\substack{j=1 \\ j\neq i}}^{n} |Y_{ij}||V_i||V_j| \sin(\theta_{ij} + \delta_j - \delta_i) \quad (2)$$

Linearising (1) and (2) about the current estimate of voltage magnitude and phase angle gives the Jacobian relation

$$\begin{bmatrix} \Delta P \\ \Delta Q \end{bmatrix} = \begin{bmatrix} J_1 J_2 \\ J_3 J_4 \end{bmatrix} \begin{bmatrix} \Delta\delta \\ \Delta|V| \end{bmatrix} \quad (3)$$

where J_1 to J_4 are the partial-derivative sub-matrices of P and Q with respect to θ and $|V|$. At each iteration k, the power mismatches

$$\Delta P_i^k = P_i^{sc} - P_i^k \ , \ \Delta Q_i^k = Q_i^{sc} - Q_i^k \quad (4)$$

are used with the Jacobian to update the state variables,

$$\theta_i^{(k+1)} = \theta_i^{(k)} + \Delta\theta_i^{(k)} \ , |V|^{(k+1)} = |V|^{(k)} + \Delta|V|^{(k)} \quad (5)$$

and the process is repeated until $|\Delta P_i|$ and $|\Delta Q_i|$ fall below a specified tolerance (10^{-4} in this study). The solution algorithm proceeds by (i) reading the bus and line data, (ii) forming the bus-admittance matrix, (iii) initialising voltage magnitudes and angles at flat-start / slack-bus values, (iv) computing the mismatch vector, (v) forming and inverting the Jacobian, (vi) updating the state, and (vii) repeating from step (iv) until convergence.

3.4 Small-Signal (Modal) Analysis and Participation Factors

With the operating point established, the non-linear differential-algebraic model of the network is linearised to the state-space form

$$\Delta\dot{x} = A\Delta x + B\Delta u \ , \Delta y = C\Delta x + D\Delta u \quad (6)$$

The eigenvalues λ of the state matrix A, obtained from $det(A - \lambda I) = 0$, occur in complex-conjugate $\lambda = \sigma \pm j\omega$ for oscillatory modes. The damping ratio and oscillation frequency associated with each mode are

$$\zeta = \frac{-\sigma}{\sqrt{(\sigma^2 + \omega^2)}} \quad (7)$$

$$f = \frac{\omega}{2\pi} \quad (8)$$

A mode is considered critical when ζ falls below an acceptable damping threshold (0.05 in this study, shown as the vertical reference line in Figures 2 and 3). To identify which generator states, and by extension which transmission corridor, contribute most strongly to a given critical mode, the participation factor of state k in mode i is computed as

$$p_{ki} = \varphi_{ki}\, \psi_{ik} \quad (9)$$

where φ_{ki} and ψ_{ik} are, respectively, the $k-th$ entry of the right eigenvector and the $k-th$ entry of the left eigenvector associated with mode i. The line joining the two generators with the highest participation factors in the critical mode is taken as the corridor conveying that mode, and is the candidate location for HVDC compensation.

3.5 HVDC Dynamic Model

A two-terminal VSC-HVDC link, comprising a rectifier and an inverter station connected by a DC line modelled as a lumped RL circuit, was embedded at the identified corridor. The firing angle α at the rectifier and the extinction angle γ at the inverter are regulated by proportional–integral (PI) current/voltage controllers, with the normal operating mode defined by $I_{dc} \geq 0$ and $\alpha_{min} \leq \alpha \leq \alpha_{max}$. The differential-algebraic equations describing the converter stations and DC line follow the standard HVDC representation used for transient-stability studies [11], [17], relating the AC-side complex power injections S$S_R = P_R + jQ_R$ and $S_I = P_I + jQ_I$ to the DC quantities V_{Rdc}, V_{Idc} and I_{dc} through the transformer tap ratios m_R, m_I and the commutating reactances at each terminal, together with the rectifier and inverter current-controller dynamics. The complete parameter list is defined in Table 1 (nomenclature).

© SEP 2026 | IRE Journals | Volume 10 Issue 3 | ISSN: 2456-8880
DOI: https://doi.org/10.64388/IREV10I3-1723169

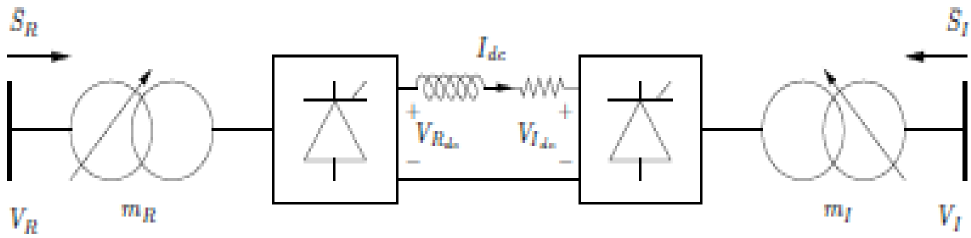

Figure 2: Model of HVDC for Voltage Stability Analysis

Table 1: Nomenclature of the HVDC dynamic model parameters.

Symbol	Description
R, I	Bus index of the rectifier and inverter stations
S_R, S_I	Complex power injected from the AC grid at the rectifier and inverter
V_R, V_I	AC primary voltage at the rectifier and inverter transformer terminals
V_{Rdc}, V_{Idc}	DC voltage at the rectifier- and inverter-side terminals
I_{dc}	DC current in the transmission line
m_R, m_I	Transformer tap ratios at the rectifier and inverter
α, γ	Firing angle (rectifier) and extinction angle (inverter)
K_P, K_I	Proportional and integral gains of the current/voltage regulators
R_{dc}, L_{dc}	Resistance and inductance of the DC line
H	Generator inertia constant
D	Machine damping coefficient
δ, ω	Rotor angle and rotor speed

3.6 Time-Domain Simulation

Transient-stability assessment requires the solution of a system of coupled non-linear differential equations for which no general closed-form solution exists. The classical machine swing equation was cast in state-variable form as

$$\frac{d\delta}{dt} = \omega - \omega_s \tag{10}$$

$$\frac{d\omega}{dt} = \left(\frac{\omega_s}{2H}\right) \cdot [P_m - P_e - D(\omega - \omega_s)] \tag{11}$$

and solved using the modified Euler (predictor–corrector) method. For a step size h, the predictor estimates are

$$X_p^{(n+1)} = X_n + h \cdot f(x_n, t_n) \tag{12}$$

and the corrected value is obtained from the average of the derivatives at the predicted and current points,

$$X_{n+1} = X_n + \left(\frac{h}{2}\right) \cdot [f(X_n, t_n) + f(X_p^{(n+1)}, t_{n+1})] \tag{13}$$

This predictor–corrector scheme was applied at every integration step to update rotor angle, rotor speed, bus voltage and line power flow throughout the simulation window.

3.7 Simulation Scenario

A solid three-phase fault was applied on the Ikeja-West–Benin 330 kV line – the corridor identified by the participation-factor analysis (Section 4.2) as conveying the critical inter-area mode. The fault was applied at $t = 0.5\ s$ and cleared at $t = 0.52\ s$ at the

© SEP 2026 | IRE Journals | Volume 10 Issue 3 | ISSN: 2456-8880
DOI: https://doi.org/10.64388/IREV10I3-1723169

Ikeja-West end and $t = 0.54\,s$ at the Benin end, consistent with typical protection-clearing sequences on the network. The total simulation window was 10 s, over which the responses of generator rotor speed, active and reactive power flow on selected lines, and bus voltage at selected buses were recorded with and without the HVDC link in service.

IV. RESULTS AND DISCUSSION

This section presents the results of the modal (eigenvalue) analysis used to site the HVDC link, followed by the time-domain simulation results with and without HVDC for rotor speed, active/reactive line power flow, and bus voltage.

4.1 Operating Point

The Newton–Raphson power-flow solution converged within the specified tolerance, giving a pre-disturbance operating point in which all 56 bus voltages lie within the normal ANSI/IEC operating band (approximately $0.90 - 1.06\,p.u.$.), confirming that the network was, at the outset, in a technically healthy steady state prior to the fault. This operating point forms the initial condition for both the modal analysis and the time-domain simulation.

4.2 Modal Analysis and HVDC Siting

Figure 3 shows the network eigenvalue map without HVDC. Several complex-conjugate mode pairs lie to the left of the $\zeta = 0.05$ damping threshold (red line), of which modes 23 and 24 ($\zeta = 0.0373, f = 0.6156\,Hz$) are the dominant inter-area pair, and modes 30/31 exhibit negative damping ($\zeta = -0.0496$), i.e. they are unstable in the linearised sense. Participation-factor computation associates the $0.62\,Hz$ mode most strongly with the generators feeding the Ikeja-West–Benin corridor, identifying this line as the appropriate location for the HVDC link. A summary of the critical modes is given in Table 3.

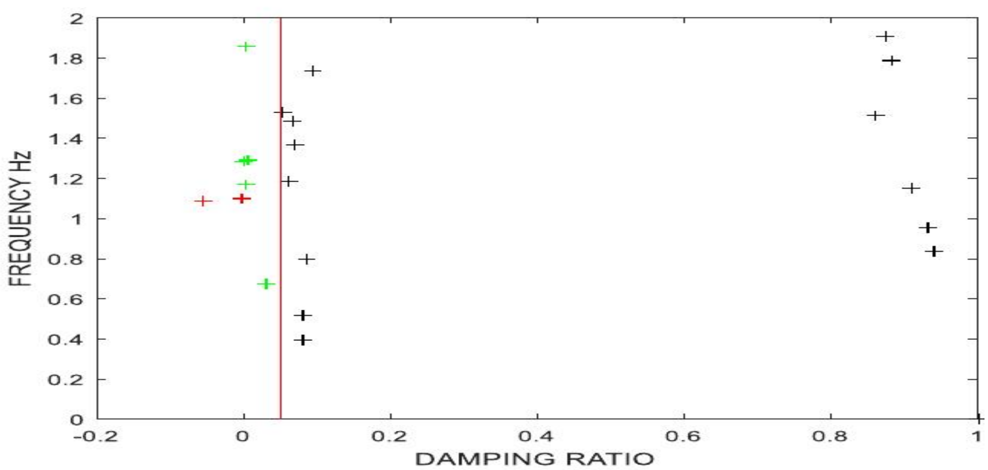

Figure 3: Network eigenvalue map without HVDC (damping ratio vs. oscillation frequency); the vertical line marks the ζ = 0.05 damping threshold.

Table 2: Critical electromechanical modes identified by eigenvalue analysis (without HVDC).

Mode No.	Damping Ratio (ζ)	Oscillation Frequency (Hz)	Classification
$23, 24$	0.0373	0.6156	Critical inter-area mode (below the 0.05 stability threshold)
$30, 31$	-0.0496	1.0004	nstable / negatively damped local mode

$16, 17$	0.0891	0.3601	Lightly damped mode, close to threshold
$19, 20$	0.0907	0.4718	Lightly damped mode, close to threshold
$59, 60 - 76, 77$	$0.86 - 0.94$	$0.83 - 1.91$	Well-damped local modes (reference only)

Following insertion of the HVDC link at the Ikeja-West–Benin corridor, the eigenvalue map shifts substantially to the right, as shown in Figure 4: the previously unstable and lightly damped modes are pulled into the stable, well-damped region, confirming that HVDC compensation at this location directly improves the damping of the modes responsible for the inter-area oscillation.0

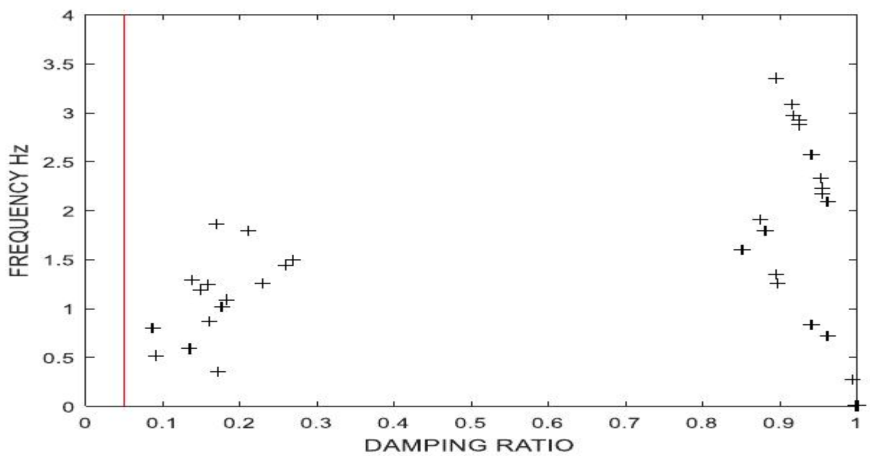

Figure 4: Network eigenvalue map with HVDC embedded at the Ikeja-West–Benin corridor.

4.3 Rotor-Speed Response

Figure 5 shows the rotor-speed response of the Egbin generating plant following the three-phase fault, with and without HVDC. Without HVDC, the rotor speed does not fully settle within the 10 s simulation window; with HVDC, the overshoot and settling time are both markedly reduced. The corresponding results for all six monitored generating stations are summarised in Table 3.

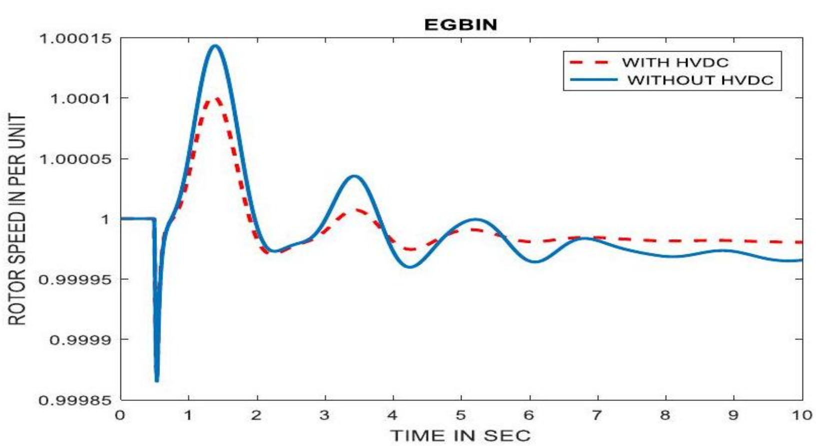

Figure 5: Rotor speed of the Egbin generating plant versus time, with and without HVDC.

Across the six stations, HVDC reduces rotor-speed overshoot by 25.0-44.4% and improves settling time by 38.0-52.0%. The comparatively smaller overshoot reduction observed at the hydro stations (Jebba, Shiroro) is consistent with the larger rotating mass/inertia of hydro turbine-generator sets, which inherently damps overshoot amplitude but is less effective at shortening the oscillation duration – the latter is where the HVDC contribution is most pronounced for these units.

Generating Station	Peak Speed w/o HVDC (p.u.)	Peak Speed w/ HVDC (p.u.)	Overshoot Reduction (%)	Settling Time w/o HVDC (s)	Settling Time w/ HVDC (s)	Settling-Time Improvement (%)
Egbin	1.00015	1.00010	44.4	> 10 (not settled)	5.5	45.0
Zungeru	1.00018	1.00011	44.4	> 10 (not settled)	5.4	46.0
AES	1.00018	1.00011	44.4	> 10 (not settled)	5.4	46.0
Delta II	1.00014	1.00010	41.4	> 10 (not settled)	6.2	38.0
Jebba	1.00016	1.00012	25.0	> 10 (not settled)	4.8	52.0
Shiroro	1.00025	1.00020	25.0	> 10 (not settled)	5.2	48.0

4.4 Active and Reactive Power-Flow Response

Figure 6 shows the real-power-flow response on the Jebba–Kainji line. As this line is relatively distant from the fault location, the simulated disturbance does not produce a severe oscillation on it even without HVDC; nevertheless, HVDC still contributes an 8% reduction in overshoot and a 29% improvement in settling time. Table 5 summarises the active- and reactive-power-flow response across the monitored lines.

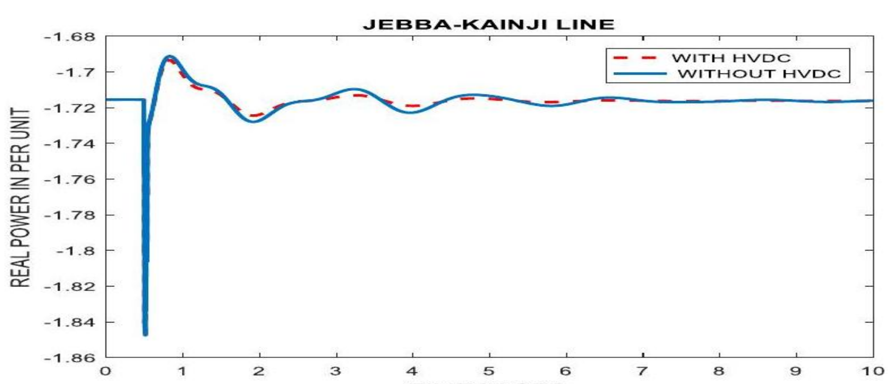

© SEP 2026 | IRE Journals | Volume 10 Issue 3 | ISSN: 2456-8880
DOI: https://doi.org/10.64388/IREV10I3-1723169

Figure 6: Real power flow on the Jebba – Kainji 330 kV line versus time, with and without HVDC.

Table 4: Summary of active- and reactive-power-flow response with and without HVDC compensation. (*peak magnitude; Δ denotes overshoot magnitude above pre-fault

Transmission Line	Parameter	Overshoot w/o HVDC (p.u.)	Overshoot w/ HVDC (p.u.)	Reduction (%)	Settling w/o HVDC (s)	Settling w/ HVDC (s)	Improvement (%)
Jebba – Kainji	Real power	-1.690	$-1.695*$	8.0	7	5	29.0
Kaduna – Kano	Real power	1.016 (Δ 0.007)	Δ 0.006	14.3	6	4	33.3
Kaduna – Jos	Real power	2.70 (Δ 0.02)	Δ 0.01	50.0	6	4	33.3
Oshogbo – Benin	Reactive power	Δ 0.010	Δ 0.007	30.0	6	4	33.3
Jebba – Kainji	Reactive power	Δ 0.010	Δ 0.006	40.0	7	4.5	35.7
Kaduna – Kano	Reactive power	Δ 0.001	Δ 0.000	100.0	4	1	75.0
Egbin – Aja	Reactive power	Δ 0.00015	Δ 0.000	100.0	6	1	83.3

The power-flow results show a clear pattern: on lightly loaded reactive-power corridors (Kaduna – Kano, Egbin – Aja) HVDC suppresses the oscillation overshoot almost completely (100%), with settling-time improvements of 75-83.3%, while on the more heavily loaded real-power corridors nearer the fault the improvement, though still material (8-50% overshoot reduction, 29-33.3% settling-time improvement), is comparatively smaller because the underlying disturbance is larger.

4.5 Bus-Voltage Response

Figure 7 shows the voltage response at the Kaduna bus, which is representative of the pattern observed at all four monitored buses: without HVDC the post-fault voltage oscillates for 6-7 s before returning to its pre-fault value, whereas with HVDC the oscillation is almost totally suppressed and the bus settles within about half a second. Table 5 summarises the bus-voltage response.

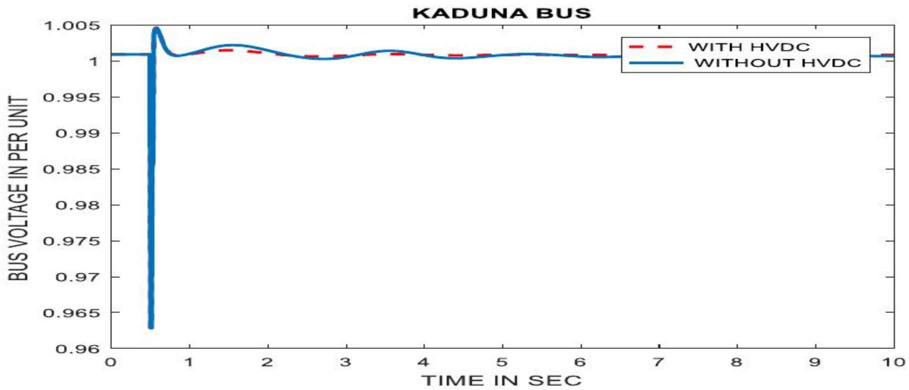

Figure 7: Bus voltage at the Kaduna bus versus time, with and without HVDC.

Table 5: Summary of bus-voltage response with and without HVDC compensation.

Bus	Pre-Fault Voltage (p.u.)	Peak Post-Fault Voltage w/o HVDC (p.u.)	Oscillation Suppression w/ HVDC (%)	Settling Time w/o HVDC (s)	Settling Time w/ HVDC (s)	Improvement (%)
Kaduna	1.002	1.005	~100 (totally suppressed)	6–7	0.54	95.0
Gombe	0.921	0.925	98.0	6	0.50	95.0
Ajaokuta	0.978	0.985	98.0	6	0.50	95.0
Ikeja-West	1.000	1.010	~100 (totally suppressed)	6	0.54	95.0

The bus-voltage results are the most striking of the four parameters monitored: oscillation is suppressed by 98-100% and settling time improves by 95% at every monitored bus, confirming that the HVDC link, once correctly sited via the modal/participation-factor procedure of Section 3.4, is highly effective at restoring voltage security across the network following a large disturbance, not only at buses electrically close to the fault.

4.6 Discussion

Taken together, the modal-analysis and time-domain results are mutually consistent: the eigenvalue shift documented in Figures 3 and 4 explains, at the linearised level, the settling-time improvements observed in the full non-linear time-domain simulation (Tables 3 – 5). This corroborates the central premise of the paper – that HVDC sited using participation-factor screening, rather than heuristically, damps the specific inter-area mode responsible for sustained oscillation on the network, rather than a mode that happens to already be well damped. Relative to the related works summarised in Table 1, the present study additionally reports the frequency (0.6156 Hz) and pre-compensation persistence (in excess of 10 s, i.e. not settled within the simulation window) of the critical mode, directly addressing the gap identified in Section 2. The results should, however, be interpreted with the following caveats: (i) the HVDC model used represents a single two-terminal link with idealised PI current/voltage regulation, and the sensitivity of the results to controller tuning was not explored; (ii) only a single fault location and clearing sequence was simulated; sensitivity to fault location, fault impedance and clearing time is a natural extension of this work; and (iii) inertia and governor/AVR data for all 56 buses were taken from the network records cited in Section 3.1 and were not independently validated against field measurements.

V. CONCLUSION

This paper has presented a modal-analysis-guided approach to siting a VSC-HVDC link for transient-stability enhancement of the Nigerian 330 kV interconnected grid. Using Newton–Raphson power flow to establish the operating point, eigenvalue and participation-factor analysis to identify the critical 0.6156 Hz inter-area mode and its associated Ikeja-West–Benin corridor, and time-domain simulation (modified Euler method) of a three-phase fault to validate the damping contribution of HVDC at that location, the study shows that all four monitored network parameters improve substantially with HVDC in service: rotor-speed overshoot reduces by up to 44.4% and settling time by up to 52%; active- and reactive-power-flow overshoot reduces by up to 100% with up to 83.3% settling-time improvement; and bus-voltage oscillation is suppressed by 98-100% with a consistent 95% settling-time improvement. These results confirm that strategically located HVDC compensation, sited using eigenvalue/participation-factor screening, is a technically effective option for mitigating inter-area oscillation and improving transient stability on the Nigerian grid.

REFERENCES

[1] G. Rogers, *Power System Oscillations*. Boston, MA, USA: Kluwer Academic Publishers, 1999.

[2] Power Holding Company of Nigeria (PHCN), *Annual Technical Report*, 2010.

[3] Power Holding Company of Nigeria (PHCN) and Energo, “Nigerian 330 kV/132 kV National Grid and Major Load Centres,” Technical Report.

[4] M. A. Almutairi and M. J. Rawa, “Transient stability analysis of large-scale PV penetration on power systems,” *Int. J. Eng. Res. Technol.*, vol. 13, no. 5, pp. 1030–1038, 2020.

[5] J. Rezaei, M. E. H. Golshan, and H. H. Alhelou, “Impacts of integration of very large-scale photovoltaic power plants on rotor angle and frequency stability of power system,” *IET Renew. Power Gener.*, vol. 16, no. 11, pp. 2384–2401, Aug. 2022, doi: 10.1049/rpg2.12529. Wiley

[6] J. Shair, H. Li, J. Hu, and X. Xie, “Power system stability issues, classifications and research prospects in the context of high-penetration of renewables and power electronics,” *Renew. Sustain. Energy Rev.*, vol. 145, Art. no. 111111, Jul. 2021, doi: 10.1016/j.rser.2021.111111. ScienceDirect

[7] F. Mesa, R. Ospina, and G. Correa, “Analysis of angular stability of the synchronous machine by biparametric bifurcations,” *J. Phys. Conf. Ser.*, vol. 1418, no. 1, 2019, doi: 10.1088/1742-6596/1418/1/012012.

[8] H. Setiadi, N. Mithulananthan, R. Shah, K. Y. Lee, and A. U. Krismanto, “Resilient wide-area multi-mode controller design based on Bat algorithm for power systems with renewable power generation and battery energy storage systems,” *IET Gener. Transm. Distrib.*, vol. 13, no. 10, pp. 1884–1894, 2019, doi: 10.1049/iet-gtd.2018.6384. Wiley

[9] R. Kumar, S. Diwania, P. Khetrapal, S. Singh, and M. Badoni, “Multimachine stability enhancement with hybrid PSO-BFOA based PV-STATCOM,” *Sustain. Comput. Inform. Syst.*, vol. 32, Art. no. 100615, Dec. 2021, doi: 10.1016/j.suscom.2021.100615. ScienceDirect

[10] Vittal, J. D. McCalley, P. M. Anderson, and A. Fouad, *Power System Control and Stability*. Hoboken, NJ, USA: Wiley, 2019.

[11] T. Abedin *et al.*, “Dynamic modeling of HVDC for power system stability assessment: A review, issues, and recommendations,” *Energies*, vol. 14, no. 16, Art. no. 4829, 2021, doi: 10.3390/en14164829. MDPI

[12] M. Sarwar *et al.*, “Stability enhancement of grid-connected wind power generation system using PSS, SFCL and STATCOM,” *IEEE Access*, vol. 11, pp. 30832–30844, Mar. 2023, doi: 10.1109/ACCESS.2023.3262172.

[13] R. Sadiq, Z. Wang, C. Y. Chung, C. Zhou, and C. Wang, “A review of STATCOM control for stability enhancement of power systems with wind/PV penetration: Existing research and future scope,” *Int. Trans. Electr. Energy Syst.*,

vol. 31, no. 11, pp. 1–27, 2021, doi: 10.1002/2050-7038.13079. Wiley

[14] X. Zhang, Z. Zhu, Y. Fu, and W. Shen, "Multi-objective virtual inertia control of renewable power generator for transient stability improvement in interconnected power system," *Int. J. Electr. Power Energy Syst.*, vol. 117, Art. no. 105641, 2020, doi: 10.1016/j.ijepes.2019.105641. ScienceDirect

[15] P. C. Gupta and P. P. Singh, "Multistability, multiscroll chaotic attractors and angle instability in multi-machine swing dynamics," *IFAC-PapersOnLine*, vol. 55, pp. 572–578, 2022, doi: 10.1016/j.ifacol.2022.04.094. ScienceDirect

[16] M. Gu, L. Meegahapola, and K. L. Wong, "Damping performance analysis and control of hybrid AC/multi-terminal DC power grids," *IEEE Access*, vol. 7, pp. 118712–118726, 2019, doi: 10.1109/ACCESS.2019.2936234.

[17] P. S. Kundur and O. P. Malik, *Power System Stability and Control*, 2nd ed. New York, NY, USA: McGraw-Hill Education, 2022. McGraw Hill

[18] C. C. Okolo, "Improving transient stability of the Nigerian 330 kV transmission system using artificial neural network based voltage source converter," Ph.D. dissertation, Nnamdi Azikiwe Univ., Awka, Nigeria, 2021.

[19] P. O. Oluseyi, T. S. Adelaja, and T. O. Akinbulire, "Analysis of the transient stability limit of Nigeria's 330 kV transmission sub-network," *Niger. J. Technol.*, pp. 213–226, 2017.

[20] L. Sundaresh, Z. Yuan, Y. Liu, and J. Pan, "Improving transient stability of interconnected power systems through HVDC controls," in *Proc. IEEE/PES Transmission and Distribution Conf. and Expo. (T&D)*, Denver, CO, USA, 2018, pp. 1–5.